MORPHOLOGICAL STUDIES OF HEPATIC TISSUE OF MICE REINFECTED WITH DENGUE VIRUS SEROTYPES 1 OR 2.

Debora Ferreira Barreto-Vieira[1], Hermann Gonçalves Schatzmayr[1], Christina Maeda Takiya[2], Fernanda Cunha Jácome[1], Manoel Enderson Vieira Silva[1], Nieli Rodrigues da Costa Faria[3], Rita Maria Ribeiro Nogueira[3], Ortrud Monika Barth[1]

[1]Laboratório de Morfologia e Morfogênese Viral, Instituto Oswaldo Cruz, Fiocruz, Rio de Janeiro.

[2]Departamento de Histologia e Embriologia, Instituto de Ciências Biomédicas, Universidade Federal do Rio de Janeiro, Rio de Janeiro.

[3]Laboratório de Flavivírus, Instituto Oswaldo Cruz, Fiocruz, Rio de Janeiro.

Corresponding author:

Debora Ferreira Barreto-Vieira, Laboratório de Morfologia e Morfogênese Viral, Pavilhão Hélio e Peggy Pereira, sala B12, Instituto Oswaldo Cruz, Fiocruz, Avenida Brasil 4365, 21040-360 Rio de Janeiro, RJ, Brazil.

Tel: +55 21 2562-1869

Fax: +55 21 2260-4866

E-mail: barreto@ioc.fiocruz.br

Key words: dengue-2 virus, dengue-1 virus, BALB/c mice, liver, ultrastructure, histopathology

ABSTRACT

Histopathological and ultrastructural aspects of liver of non-neuroadapted BALB/c mice reinfected by the intravenous route with dengue virus serotypes 1 and 2 were presented. The hepatic tissue was processed following the standard techniques for photonic and transmission electron microscopy. Morphological studies showed vacuolization of hepatocytes, inflammatory cells inside sinusoidal capillaries, enlargement of sinusoidal capillaries, foci of hemorrhage inside the interstitium, increase of surface density of reticular fibres, increase of numerical density of sinusoidal cells, decrease of surface density of hepatocytes, edema in the peri centrolobular vein space and presence of phyllopods and pseudopod-like extensions in endothelial cells. DENV particles, virus antigens and DENV RNA were observed in mosquito cells (C6/36) inoculated with sera of the animals 72 hours post-reinfection. The hepatic alterations observed in our experimental model were similar to those observed in human cases of dengue hemorrhagic fever. The present study shows that BALB/c mice reinfected with a heterologous serotype of DENV develop more severe lesions than those observed in mice in primary infection.

INTRODUCTION

Dengue fever (DF) may be caused by four serotypes of dengue viruses (DENV-1, DENV-2, DENV-3 e DENV-4), that belong to the *Flavivirus* genus, *Flaviviridae* family. The DF is the most important mosquito-borne viral disease in humans (50 to 100 million infections/year) (WHO 2002). DENV infection in humans may be subclinical or can cause two different forms of disease: DF and dengue hemorrhagic fever (DHF) and the dengue shock syndrome (DSS). DF is a self-limited febrile disease. Some patients infected with DENV develop life-threatening complications such as plasma leakage, hemorrhagic manifestations and shock (DHF/DSS) (Halstead 1981). Liver involvement in the clinical presentation of DHF (Bhamarapravati 1997, Lum et al. 1993) has been corroborated by demonstration of DENV RNA, using the reverse transcription (RT)-PCR technique, in archival liver samples obtained from individuals who succumbed to DENV infection (Rosen et al. 1999). It was speculated that the liver might be the major site of DENV replication. Studies of samples of liver obtained from patients with DHF/DSS revealed the presence of viral antigens in Kupffer cell, endothelium, lymphocytes and monocytes inside the lumen of blood vessels (Jessie et

al. 2004, De Macedo et al. 2006). It is generally accepted that DHF and the associated DSS occur as a result of secondary infection by a heterologous DENV and that immunopathological mechanisms are involved in the pathogenesis of the condition (Halstead 1970, Thein et al. 1997). Several studies suggest that mice are a permissive host for DENV (Meiklejhon et al. 1952, Lin et al. 1998, Johnson & Roehrig 1999, An et al. 1999), but in the majority of these models the animals are immunocompromised and/or inoculated by invasive routes with neuroadapted DENV in mice. Studies carried out by our group using non-neuroadapted BALB/c mice infected with DENV-2 by the intraperitoneal route, demonstrated focal alterations in the hepatic tissue. Viral antigen was detected in endothelial cells and in hepatocytes (Paes et al. 2002, 2005, Barth et al. 2006). Other mouse models, using immunocompromised mice, have documented liver involvement (Hotta et al. 1981, Chen et al. 2004). The injuries in hepatic tissue of BALB/c mice caused by DENV-1, followed by DENV-2 reinfection, using photonic and transmission electron microscopy, were characterized in the present study.

MATERIALS AND METHODS

DENV-1 and DENV-2.

The DENV-1 and DENV-2 strains were isolated in the Flavivirus Laboratory, Instituto Oswaldo Cruz, Fiocruz, from patient sera obtained in the state of Rio de Janeiro, Brazil, during the years of 2001 and 2000 respectively, and propagated in the *Aedes albopictus* mosquito cell line (C6/36). The sera were tested by the indirect immunofluorescence technique using type specific DENV-1 and DENV-2 monoclonal antibodies (DENV-1: 15F3, DENV-2: 3H5) (Henchal et al. 1982). The virus strains had undergone no passage in mouse brain. The titers of the viruses (DENV-1: $10^{7.5}$ $TCID_{50}$/0.1 mL, DENV-2: $10^{6.66}$ $TCID_{50}$/0.1 mL) were calculated by the method of Reed & Muench (1938).

Animals.

Adult male BALB/c mice, aged 2 months and weighing 25 g, were obtained from the Center of Animal Creation of the Fiocruz and maintained in the Department of Virology of the Instituto Oswaldo Cruz, Fiocruz. Mice were inoculated with DENV by the intravenous route with doses of 10,000 $TCID_{50}$/0.1 mL and euthanized 72 hours (h) post-reinfection (p.r.). The animals used as control [non-infected mice and mice inoculated with Leibovitz medium (L-15 medium)] were kept in same conditions that the infected animals. These animals were euthanized at the same day of the reinfected

animals. The experiments were divided in four groups of twenty-one animals each [ten animals reinfected with DENV and eleven control animals (non-infected and inoculated with L-15 medium)] (Table 1).

Table 1. Number of animals used in all experiments

Viruses used in primary infections	**Number of animals with clinical signs**
DENV-1	*20 animals*
DENV-2	*20 animals*
Groups with reinfection	**Number of animals in morphological studies**
Group A	*10 animals*
Group B	*10 animals*
Group C	*10 animals*
Group D	*10 animals*
Control animals (non-infected and inoculated with L-15 medium)	*44 animals*
Number of animals with morphometrical analyses	
Group A	*5 animals*
Group B	*5 animals*
Group C	*5 animals*
Group D	*5 animals*
Control animals	*5 animals*

Group A: The animals, with two months of age, were infected with DENV-2 and reinfected with DENV-1 when of four months of age.
Group B: The animals, with two months of age, were infected with DENV-2 and reinfected with DENV-1 when of six months of age.
Group C: The animals, with two months of age, were infected with DENV-1 and reinfected with DENV-2 when of four months of age.
Group D: The animals, with two months of age, were infected with DENV-1 and reinfected with DENV-2 when of six months of age.

The experiments were previously approved by the Animal Experimentation Ethical Committee of the Instituto Oswaldo Cruz, Fiocruz (number of license: P0098-01).

Blood collection.

The animals were anaesthetized and blood samples were collected in the eye plexus before the first infection and 72 hours post-infection (h.p.i.) with DENV-1 or DENV-2. Control mice samples were collected in the same time of infected animals.

Corporal temperature (primary infection).

The corporal temperature was verified in the rectal region before the first infection and 2, 6, 10 and 15 days post the first infection with DENV-1 or DENV-2. Twenty animals infected with DENV-1 or DENV-2 was used for each DENV infection assay (Table 1).

Clinical signs (primary infection).

Twenty animals infected with DENV-1 or DENV-2 was observed regarding the presence of clinical signs such as tremors, petechial, obit, diarrhea and irritability. Analyzes were executed before the first infection and 2, 6, 10 and 15 days after the first infection with DENV-1 or DENV-2. Twenty animals infected with DENV-1 or DENV-2 was used for each DENV infection assay (Table 1).

Processing of tissues for photonic microscope analysis.

The animals were euthanized 72 h.p.i and hepatic fragments were immediately collected. Animals non-infected and inoculated with L-15 medium were euthanized at the same day of reinfected mice. Samples were fixed in Millonig's fixative, dehydrated in ethanol and paraffin-embedded. Sections (5 μm thick) were stained with haematoxilyn and eosin (HE) and Gomori's silver impregnation for reticular fibres (Bancroft & Stevens 1996).

Morphometrical analysis.

Histomorphometry was performed using an imaging analysis system composed of a digital camera (Coolpix 990, NIKON, Japan) coupled to a light microscope (Eclipse 400, NIKON, Japan). Images were obtained with a 40x objective lens of a Zeiss-Axiophot photonic microscope adapted to a computational system armed of the Zeiss-AxioVision 3.0 software. All the quantifications were done on captured high quality images (2048 X 1536 pixels buffer) using the Image Pro Plus 4.5.1 software (Media Cybernetics, Silver Spring, MD, USA). A single observer performed morphological measurement blindly.

Numerical density of sinusoidal cells.

The numerical density of sinusoidal cells was obtained from histological sections of hepatic tissue from mice 72 h.p.i. stained with hematoxilyn and eosin. One hundred and thirty and six images of the five non-infected animals and one hundred and thirty and six images of liver parenchyma of the five infected animals were captured (Table 1).

Surface density of sinusoidal capillary and hepatocytes.

The surface density of sinusoidal capillary and hepatocytes was obtained from histological sections of hepatic tissue from mice 72 h.p.i. stained with hematoxilyn and eosin. One hundred and thirty and six images of the five non-infected animals and one hundred and thirty and six images of liver parenchyma of the five infected animals were captured (Table 1).

Surface density of reticular fibre.

The surface density of reticular fibers was obtained from histological sections of liver fragments from mice 72 h.p.i. stained with Gomori's method for reticular fibres (Bancroft & Stevens 1996). One hundred and thirty and six images of the five non-infected animals and one hundred and thirty and six images of liver parenchyma of the five infected animals were obtained and reticular fibers were captured (Table 1).

Statistical analysis.

Results are given as means ± standard deviation. Comparison between groups was done by one-way analysis of variance (ANOVA) or Kruskal–Wallis, and post-tested by Tukey's test. A p value of less than 0.05 was considered significant.

Processing of tissues for transmission electron microscope analysis.

The animals 72 h.p.i. were peritoneally anaesthetized and the tissue fixed by perfusion with 4% paraformaldeyde in sodium phosphate buffer (0.2M, pH 7.2) by 30 minutes. In sequence the liver tissue samples were carefully collected, post-fixed by immersion in 2% glutaraldehyde in sodium cacodylate buffer (0.2M, pH 7.2), followed by 1% buffered osmium tetroxide, dehydrated in crescent concentrations of acetone, embedded in epoxy resin and polymerized at 60^{o}C during three days. Semithin sections of 0,5 μm were obtained using a diamond knife (Diatome) adapted to a Reichert-Jung Ultracut E microtome. The sections were stained with methylene blue and azure II solution (Humprey & Pittman 1974) and observed in a Zeiss Axiophot photonic microscope. Ultrathin sections of 50-70 nm thickness were picked up onto copper grids

and stained with uranyl acetate and lead citrate (Reynolds 1963) and observed in a Zeiss EM-900 transmission electron microscope.

Isolation of DENV in the C6/36 cell line inoculated with sera from reinfected BALB/c mice.

Cell monolayers were inoculated with 100 μL of serum from mice 72 h.p.i. and incubated for 1 h at 28°C for virus adsorption. Subsequently monolayers were grown in L-15 medium supplemented with 1% non-essencial aminoacids, 10% tryptose phosphate broth, and 10% fetal bovine serum. The tubes were kept at 28°C and observed daily for viral cytopathic effects for 15 days. C6/36 normal cell monolayers was used as negative control, while the positive control consisted of cell monolayers inoculated with DENV-1 and DENV-2. After the periods of observation, the monolayers were divided into two groups; the first was tested using the indirect immunofluorescence technique (Henchal et al. 1982) with a type-specific monoclonal antibody for dengue virus (DENV-1: 15F3, DENV-2: 3H5), and the second was fixed in 1% buffered glutaraldehyde, dehydrated and embedded in epoxy resin as described above for analysis in a transmission electron microscope.

RNA extraction.

The viral RNA was extracted from C6/36 cell cultures inoculated with positive sera identified by the indirect immunofluorescence technique using a QIAmp Viral RNA Mini Kit (Qiagen, Inc., Valencia, CA, USA) according to the manufacturer's protocol.

Reverse transcription (RT-PCR).

Detection and typing of DENV in C6/36 cell culture fluids was carried out according to Lanciotti et al. (1992). This protocol detects the four serotypes of DENV simultaneously in a semi-nested procedure, generating amplified (amplicons) products with specific sizes (in bp) for each serotype of the DENV.

RESULTS

All mice of the four experimental groups survived until 72 h.p.r. with DENV-1 or DENV-2, when they were euthanized. No obit was observed in infect animals.

Analyses of clinical signs in primary infection.

Clinical signs were observed in some animals during in the first infection with DENV-1: tremors [three animals in the tenth day post-infection (d.p.i.)], irritability (five animals in the tenth d.p.i.), diarrhea (two animals, one in the second d.p.i. and the other

in the tenth d.p.i.). Animals infected with DENV-2 only did not present clinical signs as well as non-infected animals.

An increase in corporal temperature was observed in some animals of both groups of the first infection with DENV-1 or DENV-2 (Table 2). Increased temperature was observed up to 10 d.p.i. in both groups of infected animals and the first with DENV-2 infected group was more affected than DENV-1 infected mice.

Table 2. Corporal temperature of BALB/c mice infected with DENV.

VIRUS	b.i. (*)	2 d.p.i. (*)	6 d.p.i. (*)	10 d.p.i. (*)	15 d.p.i. (*)
DENV-1 n=20	2/20	4/20	1/20	1/20	0/20
DENV-2 n=20	7/20[(α)]	16/20	14/20	6/20	0/20

(*): Animals with corporal temperature above of 37^0C/ total number of animals analyzed
n= total number of animals
b.i.: before infection
d.p.i: days post-infection
[(α)]: The temperature of three animals was 37.1^0C.

Morphology.

Liver of mice non-infected and inoculated with only Leibovitz culture medium, did no exhibit any modifications in their morphology.

The alterations observed in hepatic tissue had been more severe in animals of the groups A and B (Table 3).

Table 3. Morphological alterations of liver tissue of BALB/c mice reinfected with DENV-1 and DENV-2.

Tissue alterations	*Group A*	*Group B*	*Group C*	*Group D*
Inflammatory infiltrate	**XXX**	**XXX**	**X**	**X**
Oedema	**XXXX**	**XXX**	**-**	**-**
Thrombosis	**XXXX**	**XXX**	**-**	**-**
Foci of hemorrhage	**XXXX**	**XXX**	**X**	**X**
Enlargement of bile canaliculus	**XXX**	**XXX**	**X**	**X**
Vacuolization of hepatocyte	**XXX**	**XXX**	**X**	**X**
Steatosis	**XXX**	**XXX**	**X**	**X**
Production of elastic fibres	**XXX**	**XX**	**XXXX**	**XX**
Dilatation of sinusoidal capillaries	**XXXX**	**XXX**	**XX**	**XX**
Increase of numerical density of sinusoidal cells	**X**	**XXX**	**XX**	**XX**
Necrosis of hepatocytes	**XXX**	**XX**	**X**	**X**

-: alterations not observed
X: focal alterations
XX: light alterations
XXX: moderate alterations
XXXX: strong alterations

Group A. Histopathology of liver tissue showing edema, inflammatory infiltrate and dilated lymphatic vessel in the portal space (Figs. 1a-b), portal vein containing one dilated sinusoidal capillary (Fig. 1c), some erythrocytes presenting morphological alterations (Fig. 1d), inflammatory infiltrate in the interstitium, focus of haemorrhage and increased reticulin network (Fig. 1e). Ultrastructural analysis showed enlargement of bile canaliculi and hepatocytes with dilatation of the rough endoplasmic reticulum and lipid inclusions inside the cytoplasm.

Group B. The liver of these animals showed hepatocytes with microvesicular steatosis and glycogen particles inside the cytoplasm (Fig. 2a); some cells showed vacuolization and rarefied cytoplasm (Fig. 2b). Multivesicular stellate cells presenting electron-dense (Fig. 2d) and lucid lipid vesicles in the space of Disse and synthesizing collagen were observed. Endothelial cells of the sinusoidal capillaries showed alterated phyllopod membranes which pseudopod-like extensions (Fig. 2c).

Group C. These animals showed discreet vacuolization of hepatocytes (Fig. 1f) with inflammatory infiltrate in the peri-portal space (Fig. 1g). Ultrastructural analysis of hepatocytes showed degranulation and dilation of the rough~~-surfaced~~ endoplasmic reticulum, lipid inclusions and dilation of the bile canaliculi presenting electron-dense filamentous material (Fig. 2e).

Group D. These animals presented discreet vacuolization of hepatocytes ~~with~~ and inflammatory infiltrate in the peri-portal space. Ultrastructural analysis showed endothelial cells of sinusoidal capillaries with phyllopods and electron-dense material inside the cytoplasm, enlargement of bile canaliculi, some hepatocytes with dilatation and alteration of mitochondria cristae. Ultrastructural analysis of hepatocytes showed degranulation and dilation of the rough~~-surfaced~~ endoplasmic reticulum and lipid inclusions inside the cytoplasm (Fig 2f). The morphological alterations observed in this group were less severe than in the group C.

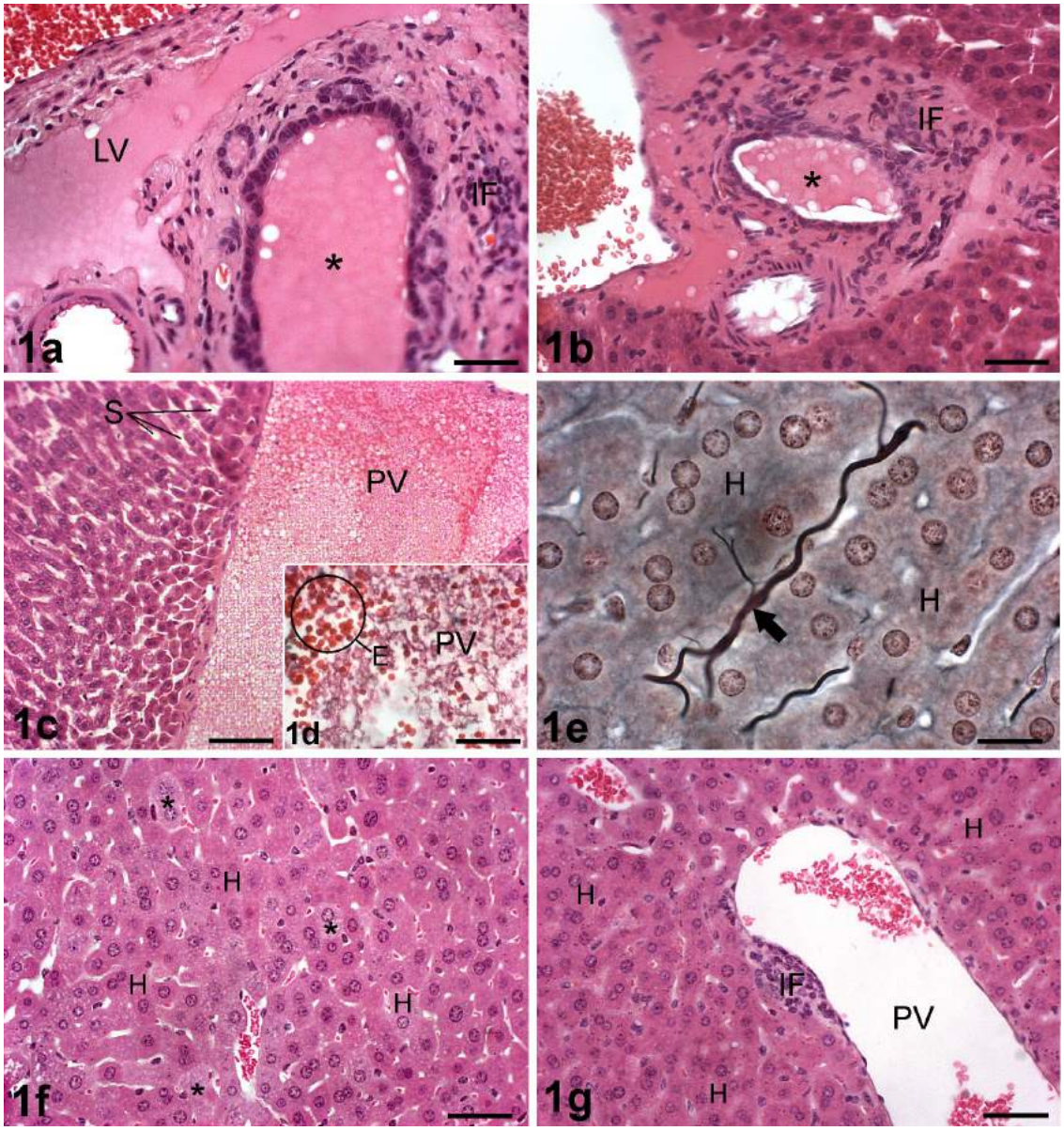

Figure 1. Figs. 1a-b: Section of mouse liver of group A showing portal space. Note oedema (*), inflammatory infiltrate (IF) and dilated lymphatic vessel (LV). HE staining. A: Bar= 40µm, B: Bar= 50µm. **Figs. 1c-d:** Section of mouse liver of group A. Note portal vein (PV) containing deformed erytrocytes (E) and dilated sinusoidal capillaries (S). HE staining. C: Bar= 50µm, D: Bar= 50µm. **Fig. 1e:** Section of mouse liver of group A showing groups of reticulin fibers (arrow) inside the sinusoidal capillaries. Hepatocyte (H). Reticulin staining. Bar= 40µm. **Fig. 1f:** Hepatic tissue of animal of group C showing some hepatocytes with light vacuolization (*). Hepatocytes (H). HE staining. Bar= 50µm. **Fig. 1g:** Hepatic tissue of group C presenting inflammatory infiltrate (IF) in the peri-portal (PV) space. Hepatocytes (H). HE staining. Bar= 50µm.

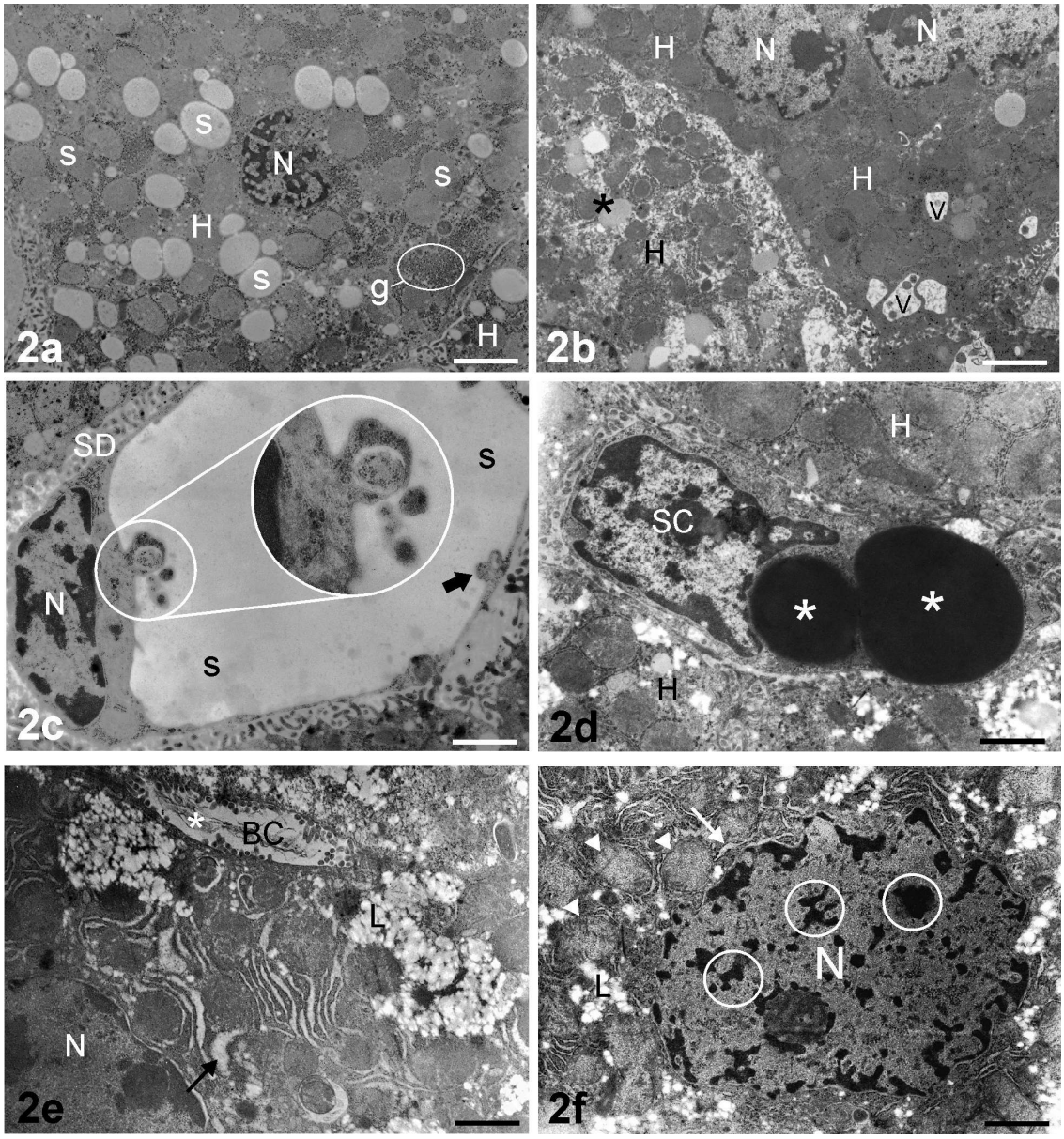

Figure 2. Fig. 2a: A hepatocyte (H) of mouse of group B presenting microvesicular steatosis (s) and some glycogen particles (circle) inside the cytoplasm. Nucleus (N), glycogen (g). Bar= 1.8 µm. **Fig. 2b:** Three hepatocytes (H) of mouse of group B showing vacuolization (V) and rarefied cytoplasm (*) of one them. Nucleus (N). Bar= 2 µm. **Fig. 2c:** Endothelial cell of mouse of group B presenting membrane alterations (arrow) wich pseudopod-like extensions. Space of Disse (SD), sinusoidal capillary (S) nucleus (N). Bar= 1.2 µm. **Fig. 2d:** Hepatic tissue mouse of group D presenting multivesicular stellate cells (SC) with some electron-dense (*) vesicles. Hepatocyte (H). Bar= 1.2 µm. **Figs. 2e-f:** Hepatocytes of group C and group D (respectively). Note degranulation and dilation (arrow) of rough-surfaced endoplasmic reticulum, lipid inclusions (L), presence of electron-dense filamentous material (*) inside bile canaliculus (BC), swollen of mytochondria (arrow heat) and chromatin clumps (circle). Nucleus (N). E-F: Bar= 1 µm.

Morphometry.

Average of the suface density of hepatocytes. A decrease of the surface density of hepatocytes in all groups of reinfected mice was verified in relation to the control group (Graphic 1). In the group A (two months old animals infected with DENV-1 and reinfected with DENV-2 when four months aged) the decrease was greater than in the other groups. The difference between group C ((two months old animals infected with DENV-1 and reinfected with DENV-2 when four months aged)) and the control group was only 1.55%.

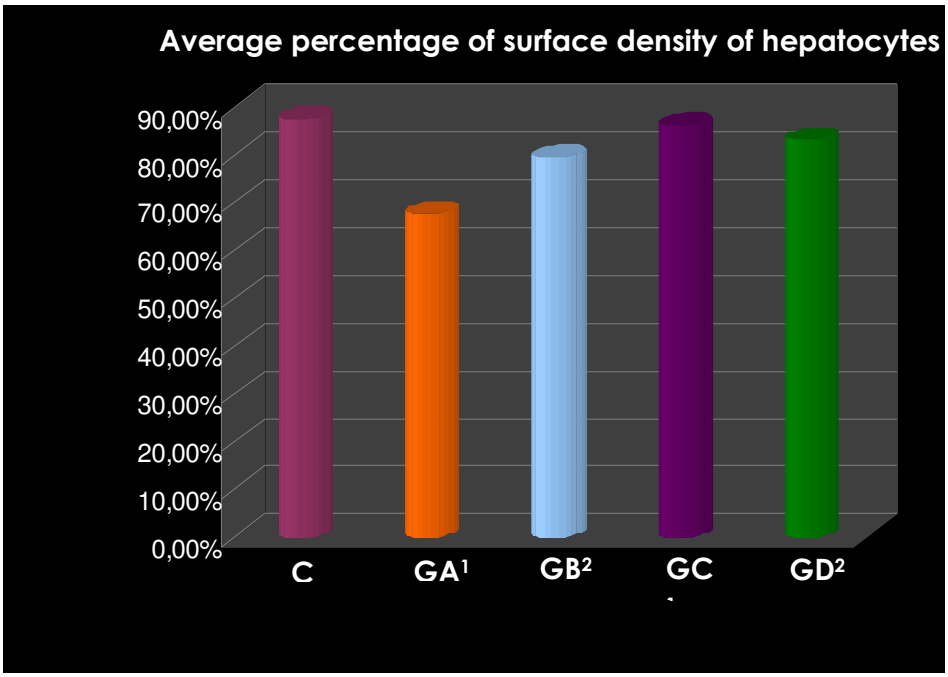

Graphic 1. Average percentage of suface density of hepatocytes of BALB/c mice infected and reinfected with DENV serotypes 1 or 2. N= 136 images per group.

Average of the surface density of elastic fibres of liver. A significant increase of the surface density of elastic fibres was verified in all groups of reinfected mice in relation to the control group (Graphic 2). Its increase in the group C (two months old animals infected with DENV-1 and reinfected with DENV-2 when four months aged) was greater than in the other groups.

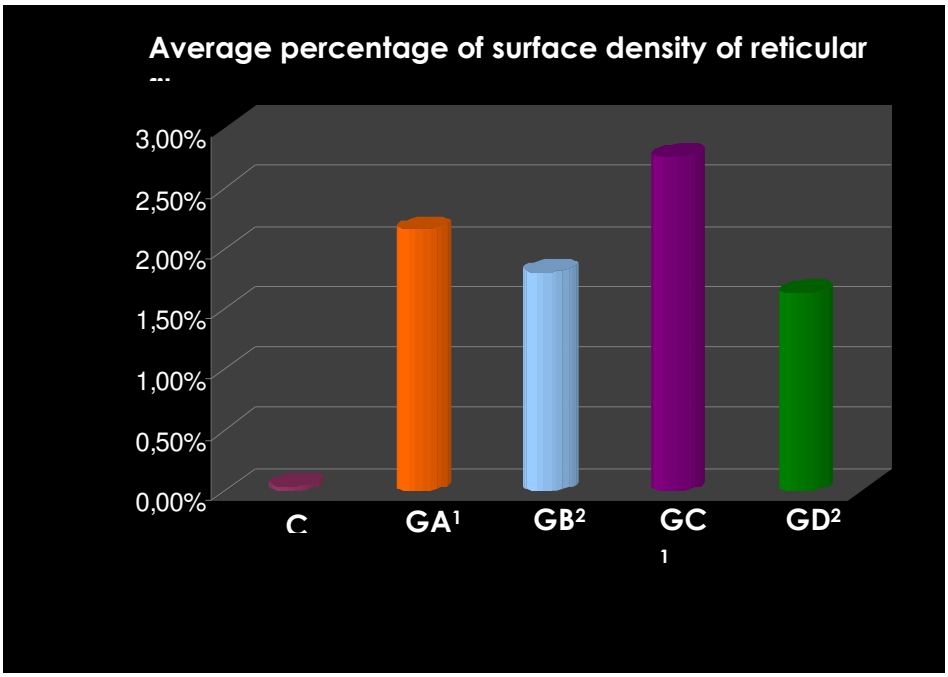

Graphic 2. Average percentage of surface density of elastic fibres of BALB/c mice infected and reinfected with DENV serotypes 1 or 2. N= 136 images per group.

Average of the surface density of sinusoidal capillaries.

An increase of the surface density of sinusoidal capillaries was observed in all groups of reinfected mice in relation to the control group (Graphic 3). In the group A (two months old animals infected with DENV-2 and reinfected with DENV-1 when four months aged) the increase was greater than in the other groups (32.50%). The difference between group C (two months old animals infected with DENV-1 and reinfected with DENV-2 when four months aged) and the control group was only 1.35%.

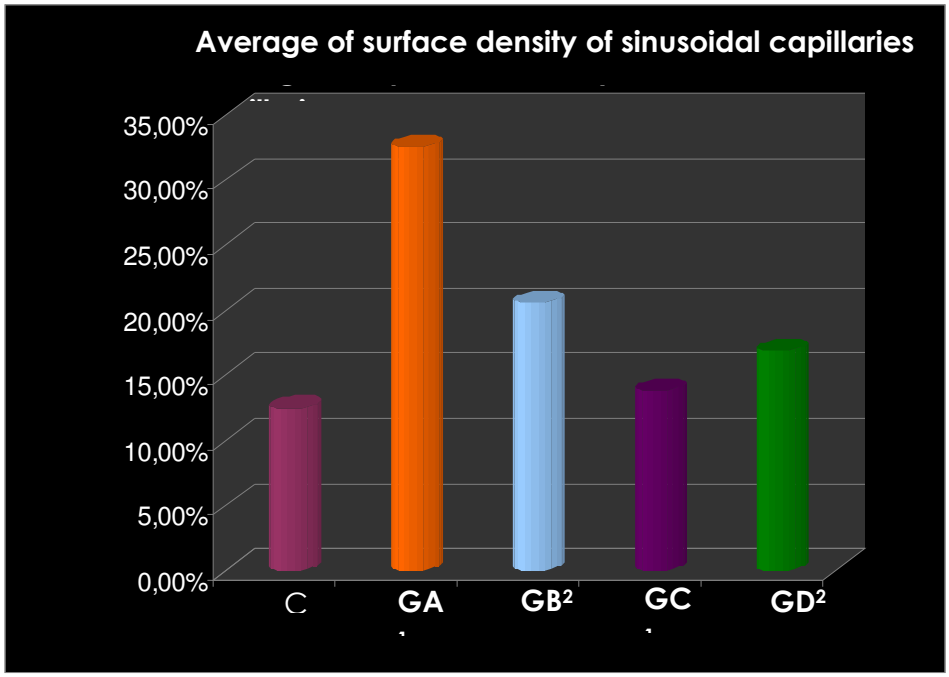

Graphic 3. Average percentage of surface density of sinusoidal capillaries of BALB/c mice infected and reinfected with DENV serotypes 1 or 2. N= 136 images per group.

Average of the numerical density of sinusoidal cells. An increase of the numerical density of sinusoidal cells was verified in all groups of reinfected mice in relation to the control group (Graphic 4). In the B group (two months old animals infected with DENV-2 and reinfected with DENV-2 four months later) the increase ~~it~~ was greater than in the other groups. The difference between group A (two months old animals infected with DENV-2 and reinfected with DENV-1 when four months aged) and the control group was very small (only 1 cell more for image).

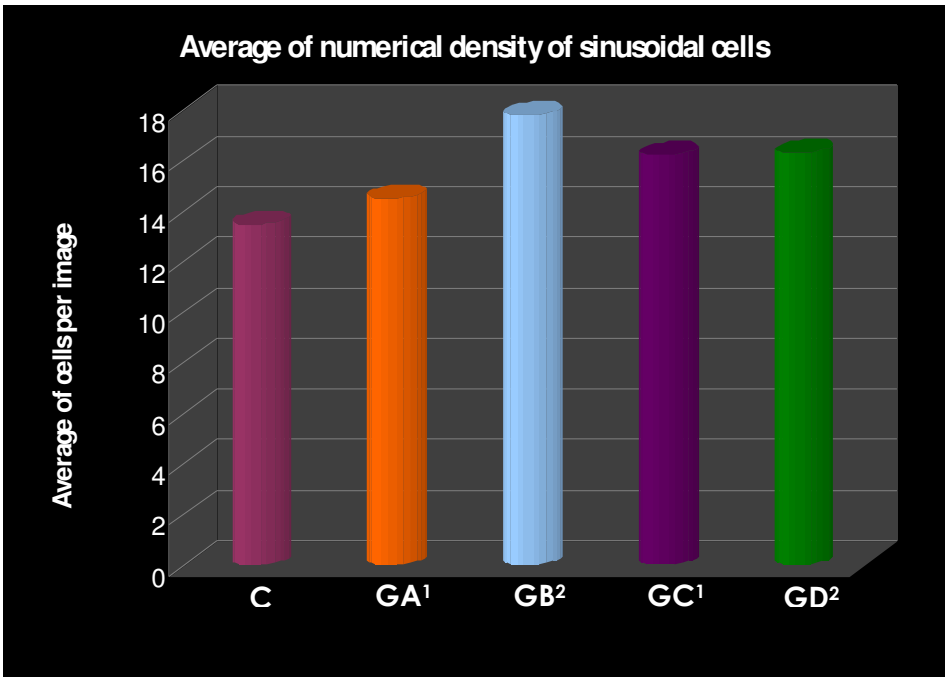

Graphic 4: Average percentage of numerical density of sinusoidal cells of BALB/c mice infected and reinfected with DENV serotypes 1 or 2. N= 136 images per group. C: control, GA: group A, GB: group B, GC: group C, GD: group D.[1]: first infection with 2 months of age and second infection with 4 months of age, [2]: first infection with 2 months of age and second infection with 6 months of age. The percentage in grafics 1, 2 and 3 was express in μm^2.

Detection of DENV in the C6/36 cell line inoculated with sera from reinfected BALB/c mice.

The syncytial cytophatic effect started to be visible around the 13th day post-infection in monolayers of the C6/36 cells of positive control and in the cultures inoculated with the strain of serum of reinfected animals. At the 15th d.p.i., monolayer cells of the negative control showed no morphological alterations, exhibited neither DENV antigen and nor virus particles. In positive control cell cultures and in monolayer cultures inoculated with sera of A and B group animals, the DENV-2 antigen was observed by the indirect immunofluorescence technique (Figs. 3a-b). The presence of a syncytial cytophatic effect was observed in all monolayers. Ultrastructural observations of cell cultures of the positive controls and in monolayer cultures inoculated with ~~the~~ sera showed virus particles inside cytoplasmic vesicles (Fig. 3c) and immature particles in cysterns of the rough endoplasmic reticulum (Fig. 3d). All cell monolayers inoculated with sera of group C and D animals contaminated, hampering the viruses isolation.

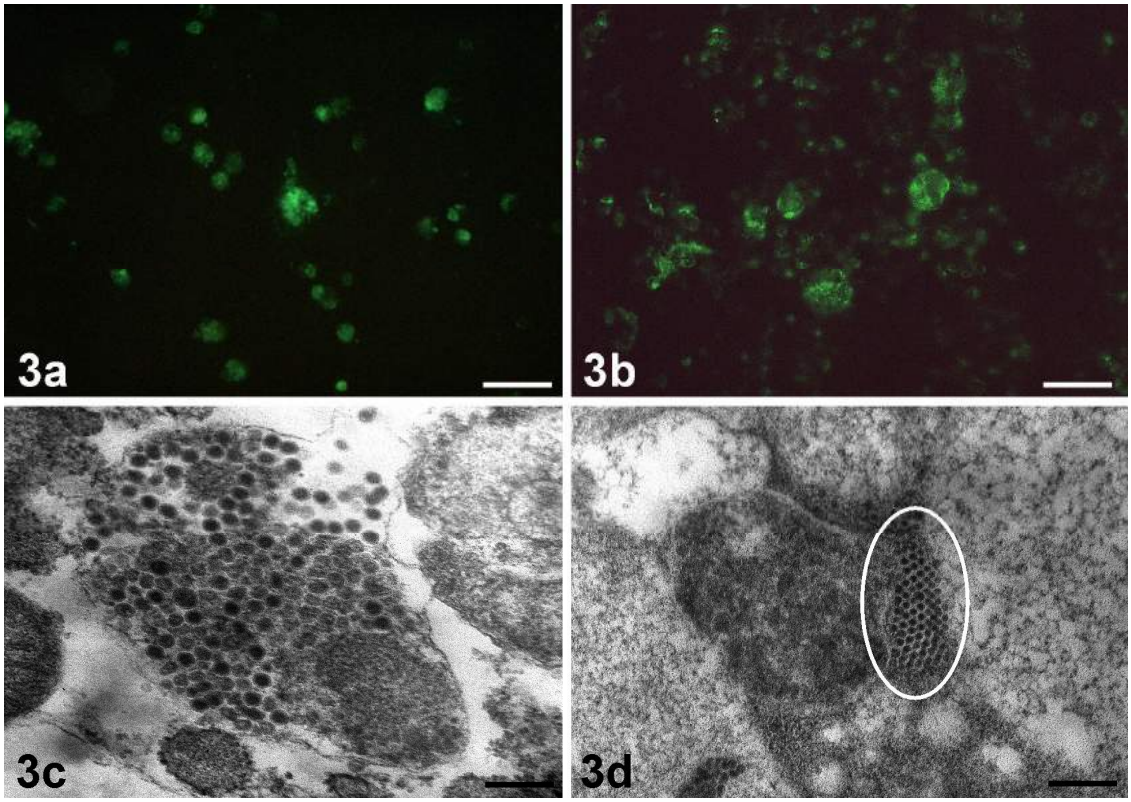

Figure 3. Figs. 3 a-d: Detection of DENV antigen and virus particles in monolayers of C6/36 cells. a-b: Presence of DENV-1 antigen in cell monolayer inoculated with serum of an animal of the group A. Immunofluorescence technique (a-b: Bar= 1.25 μm) ; c: Presence of DENV-1 particles inside a cytoplasmic vesicle of a C6/36 cell culture inoculated with serum mouse of group B (Bar= 0.1 μm); d: presence of incomplete DENV-1 particles inside the lumen of the rough endoplasmic reticulum (ellipse) of a C6/36 cell culture inoculated with serum of mouse of group A (Bar= 0.3 μm). Transmission electron microscopy technique.

Detection of DENV viral genome by RT-PCR.

The genome of DENV-1 was detected in extracts of C6/36 cells inoculated with mouse sera of A and B groups collected at the 72 h.p.r. (Fig. 4). No genome was observed in monolayers of the negative control. These results confirmed the presence of DENV-1 in serum samples of reinfected mice and indicated that such virus is still able to infect other cells.

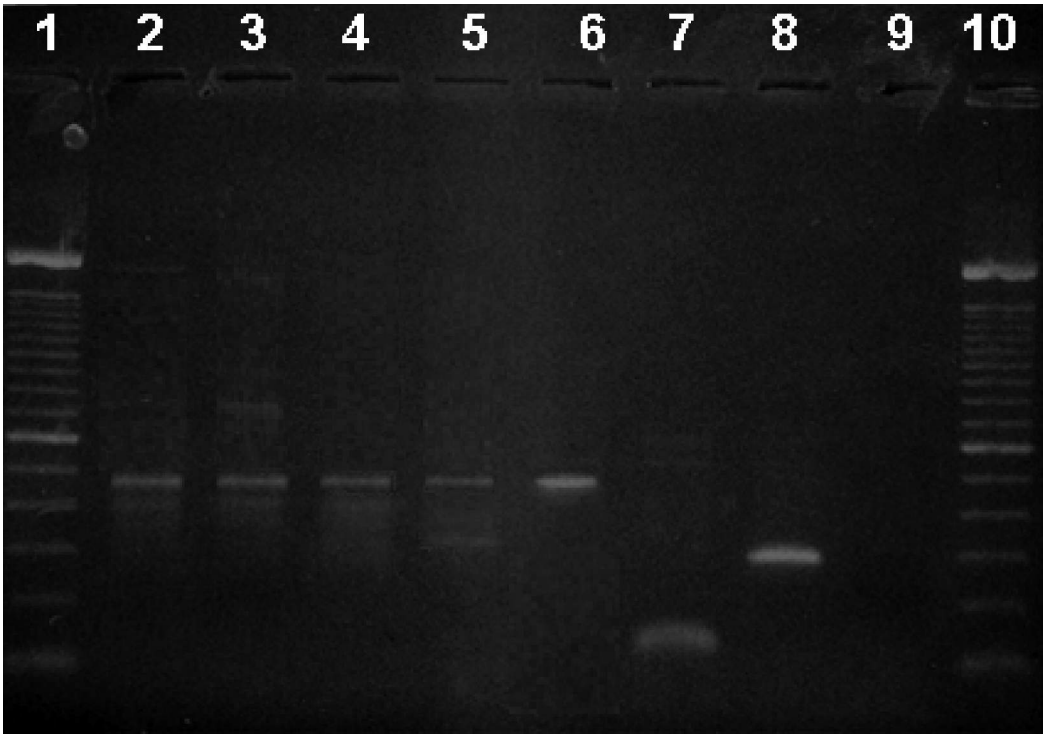

Figure 4. Fig. 4: RT-PCR of extracts of C6/36 cells inoculated with mouse sera of the group A and group B. Lines 1/10: 100-bp, ladder (Gibco). Lines- 2/4: C6/36 cells inoculated with strain of serum of BALB/c mice of the B group; 3/5: C6/36 cells inoculated with strain of serum of BALB/c mice of the A group; 6: DENV-1 positive control; 7: DENV-2 positive control; 8: DENV-3 positive control; 9: Negative control (H_2O).

DISCUSSION

The lack of an appropriate animal model for dengue virus has hundered a better characterization of the mechanisms underlying the disease pathogenesis (Shresta et al. 2006). Studies demonstrated that nonobese diabetic/severely compromised immunodeficient (NOD/SCID) mice, xenografted with CD34+ cells, developed clinical signs of DF as in humans (fever, rash and thrombocytopenia) (Bente et al. 2005). The majority of animal models used immunodeficient mice inoculated by invasive routes with neuroadapted mouse DENV strains (Nath et al. 1983, Raut et al. 1996). Mice in the great majority of these models, exhibited paralysis and developed thrombocytopenia. The objective of the present study was to develop a murine model that better resembles human DHF/DSS disease. Animals reinfected with a heterologous serotypes (non-neuroadapted strains of DENV-1 and DENV-2) by the intravenous route presented alterations in hepatic tissue similar with human cases of DHF/DSS. The morphological alterations observed has been more severe than those observed in our previous works

(Barreto et al. 2002, 2004, 2007, Barth et al. 2006) in which the animals were infected only with one serotype of DENV.

The normal dengue infection response changed to a more severe disease in some individuals that showed pre-infection dengue antibodies. The reaction occurs more frequently in individuals with secondary infection by DENV-2 (Halstead 1970, Rajapakse 2011). Different of the human dengue infection cases, our animal model showed more severe injuries in hepatic tissues of mice reinfected with DENV-1. Mice submitted to a second heterotypic dengue virus (DENV-2) presented severe infection (Sarkar et al. 1976).

Hepatic involvement in dengue virus infections has been documented (Havens 1954). Dengue antigen has been identified within Kupffer cells, endothelium, lymphocytes and monocytes inside the lumen of sinusoidal capillaries of individuals presenting DF, DHF or DSS (Guzman et al. 2002, Jessie et al. 2004). Studies reported fatal hepatic failure in an adult arising as a complication of DHF (Lawn et al. 2003, Ling et al. 2007). Liver histology revealed marked steatosis and a florid hepatitis with necrosis. Similar alterations were observed in the present study. Hepatocyte alterations were verified by morphometrical analyses that showed a decrease of its superficial density in all reinfected animals (groups A-D), as well as microvesicular steatosis. Liver dysfunction, as a result of dengue infection, may be a direct viral effect on liver cells or an adverse consequence of dysregulated host immune responses against the virus (Seneviratne et al. 2006).

Fibrosis is a frequent, life-threatening complication of most chronic liver diseases (Gressner et al. 2007). Massive calcification in liver was observed in patients with dengue virus-associated fulminant liver failure (Saikia et al. 2007, Fabre et al. 2001). Our analyses of reinfected animals presented multivesicular stellate cells storing electron-dense and lucid lipid vesicles and secreting collagen into the Disse space. Morphometrical analyses showed increase of superficial density of reticular fibres. Infiltrate of inflammatory cells was observed in all the groups of reinfected animals, being the most proeminent in the groups A and B. Current knowledge ascribes to liver-specific pericytes, conferring to hepatic stellate cells a major role in extracellular matrix production and re-modelling (Pinzani 1995, Gressner & Bachem 1995, Gressner 1996, Gressner & Weiskirchen 2006). Its dominant role in fibrogenesis is based on their ability to change the phenotype from retinoid-storing, resting cells to contractile, smooth-muscle α-actin positive, vitamin A-depleted myofibroblasts with a strongly

developed endoplasmic reticulum and Golgi-apparatus, when hepatic stellate cell were challenged by necro-inflammatory stimuli (Bataller & Brenner 2005, Friedman 2004).

As the endothelium forms the primary barrier of the circulatory system, dysfunction of the endothelial cells during acute diseases can broadly affect vascular permeability and cause plasma leakage (Lee et al 2006). In our mouse model the endothelial cells of sinusoidal capillaries exhibited phyllopodia, alterations of cytoplasm membranes (blebs) and vacuoles of secretion. Necrosis of this cellular type was not observed. According to Feroze (1997), the presence of a great number of endocytic vacuoles and phyllopodia in endothelial cells can be an indicative of cell activation. Researchers have suggested that endothelial cells can support DENV replication and liberation of several inflammatory mediators including interleukin 8 (IL-8) and RANTES (Avirutnan et al. 1998, Juffrie et al. 2000). These substances are capable to enlist neutrophiles and to promote vascular permeability increase. Foci of hemorrhage and edema were observed in the present experiments,-probably due to the release of IL-8 and RANTES by activated endothelial cells.

The bile canaliculi showed dilation, presence of electron-dense filamentous material inside and loss of microvilli in the present ultrastructural analysis. Loss of microvilli, formation of surface membrane blebs and disorganization of the pericanalicular actin filament web are common features in many forms of cholestasis (Scheuer & Lefkowitch 2000). In the cholestasis related to preservation injury after liver transplantation, for example, ischaemia and reperfusion injury result in canalicular dilatation, loss of microvilli and compactation of actin filaments (Cutrin et al. 1996).

The endoplasmic reticulum is an important site of protein synthesis and transport. It also contains enzymes involved in drug and steroid metabolism. Several endogenous imbalances in cells, such as massive protein production, loss of calcium homeostasis, inhibition of N-linked glycosylation, and accumulation of mutant protein, often contribute to its malfunction (Yu et al. 2006). One of the major morphological changes in Flavivirus-infected cells is the proliferation and hypertrophy of endoplasmic reticulum membranes, where virus particles accumulate inside (Barth 2000, Burke & Monath 2001, Hase et al. 1992). We observed hepatocytes with degranulation and dilation of the rough endoplasmic reticulum. Lipid inclusions were observed inside these cells also.

Several studies utilizing mice as an experimental model for DENV infection have been carried out. The susceptibility of BALB/c mice inoculated with neuroadapted

DENV by intraperitoneal and intravenous route in primary infection was demonstrated (Atrasheukaya et al. 2003, Huang et al. 2000). In present study, DENV-1 was ultrastructurally indentified and immunolocalized and RNA detected in extracts of C6/36 cell cultures inoculated with serum of BALB/c mice 72 h.p.r. Ultrastructural studies showed the presence of DENV particles inside cytoplasmic vesicles and immature particles in cisterns of the rough endoplasmic reticulum. These findings confirm that BALB/c mice are susceptible for infection and re-infection by DENV-1 or DENV-2 and that they are capable to develop morphological alterations similar to those observed in human cases of dengue hemorrhagic fever.

ACKNOWLEDGMENTS

To the staff of the Flavivirus Laboratory of the Departament of Virology for virus isolation and identification, to the Department of Pathology and to the Laboratory of Image Processing of the Instituto Oswaldo Cruz; to Ms. Ana Paula Alves Silva for technical assistance. Financial support: CNPq, Faperj.

References

An J, Kimura-Kuroda J, Hirabayashi Y, Yasui K 1999. Development of novel mouse model for dengue virus infection. *Virology* 263: 70-77.

Atrasheuskaya A, Petzelbauer P, Fredeking TM, Ignatyev G 2003. Anti-TNF antibody treatment reduces mortality in experimental dengue virus infection. *FEMS Immunol. Med. Microbiol.* 35: 33-42.

Avirutnan P, Malasit P, Seliger B, Bhakdi S, Husman M 1998. Dengue virus infection in human endothelial cells leads to chemokine production, complement activation and apoptosis. *J. Immunol.* 161: 6338-6346.

Bancroft JD & Stevens A 1996. Theory and practice of histological techniques. Churchill Livingstone, New York, Fourth edition, 766 p.

Barreto DF, Paes MV, Takiya CM, Pinhão AT, Côrtes LMC, Majerowicz S, Barth OM 2002. Mice lung experimentally infected with dengue-2 virus: ultrastructural aspects. *Virus Rev. & Res.* 7: 47-55.

Barreto DF, Takiya CM, Paes MV, Farias-Filho J, Pinhão AT, Alves AMB, Costa SM, Barth OM 2004. Histopathological aspects of dengue-2 virus infected mice tissues and complementary virus isolation. *J. Submicrosc. Cytol. Pathol.* 36: 121-130.

Barreto DF, Takiya CM, Schatzmayr HG, Nogueira RMR, Farias-Filho J, Barth OM 2007. Histopathological and ultrastructural aspects of mice lung experimentally infected with dengue virus serotype 2. *Mem. Inst. Oswaldo Cruz* 102: 175-182.

Barth OM 2000. Atlas of dengue viruses morphology and morphogenesis. Imprinta Express Ltda., Rio de Janeiro. 209 p.

Barth OM, Barreto DF, Pinhão AT, Takiya CM, Paes MV, Shatzmayr HG 2006. Morphological studies in model for dengue-2 virus infection in mice. *Mem. Inst. Oswaldo Cruz* 101: 905-915.

Barreto-Vieira DF, Barth-Schatzmayr OM, Schatzmayr HG 2010. Modelo animal experimental para o estudo da patogênese dos vírus dengue sorotipos 1 e 2. Manual de Técnicas. Editora Interciência, Rio de Janeiro. 82 p.

Bataller R, Brenner DA 2005. Liver fibrosis. *J. Clin. Invest.* 115: 209-218.

Bente DA, Melkus MW, Garcia JV, Rico-Hesse R 2005. Dengue fever in humanized NOD/Scid Mice. *J. Virol.* 79: 13797-13799.

Bhamarapravati N 1997. Pathology of dengue infections. In: DJ Gubler, G Kuno (eds.). Dengue and dengue hemorrhagic fever. CAB International, New York, p. 115-132.

Burke DS, Monath TP 2001. Flaviviruses. In: DM Knipe and PM Howley (eds.). Fields Virology, 4th ed., vol. 1. Lippincott-Williams & Wilkins, Philadelphia, Pa, p. 1043-1125.

Chen HC, Lai SY, Sung JM, Lee SH, Lin YC, Wang WK, Chen YC, Kao CL, King CC, Wu-Hsich BA 2004. Lymphocyte activation and hepatic cellular infiltration in immunocompetent mice infected by dengue virus. *J. Med. Virol.* 73: 419-431.

Cutrin JC, Cantino D, Biasi F 1996. Reperfusion damage to the bile canaliculi in transplanted human liver. *Hepatology* 24: 1053-1057.

De Macedo FC, Nicol AF, Cooper LD, Yearsley M, Pires AR, Nuovo GJ 2006. Histologic, viral, and molecular correlates of dengue fever infection of the liver using highly sensitive immunohistochemistry. *Diagn. Mol. Pathol.* 15: 223-228.

Fabre A, Couvelard A, Degott C, Lagorce-Pages C, Bruneel F, Bouvet E, Vachon F 2001. Dengue virus induced hepatitis with chronic calcific changes. *Gut* 49: 864-865.

Feroze NG 1997. Ultrastructural pathology on the cell and matrix, 4th ed., p. 619-1414.

Friedman SL 2004. Mechanisms of disease: mechanisms of hepatic fibrosis and therapeutic implications. *Nat. Clin. Pract. Gastr.* 1: 98–105.

Gressner AM 1996. Transdifferentiation of hepatic stellate cells (Ito cells) to myofibroblasts: a key event in hepatic fibrogenesis. *Kidney Int.* 49: S 39–45.

Gressner AM, Bachem MG 1995. Molecular mechanisms of liver fibrogenesis - a homage to the role of activated fat-storing cells. *Digestion* 56: 335–346.

Gressner AM, Weiskirchen R 2006. Modern pathogenetic concepts of liver fibrosis suggest stellate cells and TGF-beta as major players and therapeutic targets. *J. Cell Mol. Med.* 10: 76–99.

Gressner OA, Weiskirchen R, Gressner AM 2007. Biomarkers of hepatic fibrosis, fibrogenesis and genetic pre-disposition pending between fiction and reality. *J. Cell Mol. Med.* 11: 1031-1051.

Guzman MG, Kouri G 2002. Dengue: an update. *Lancet Infect. Dis.* 2: 33-42.

Halstead SB 1970. Observations related to pathogenesis of dengue haemorrhagic fever. VI. Hypotheses and discussion. *Yale J. Bio. Med.* 42: 350.

Halstead SB 1981. Dengue haemorrhagic fever - a public health problem and field for research. *Bull. WHO* 58: 1-21.

Hase T, Summers PL, Ray P, Asafo-Adjei E 1992. Cytopathology of PC12 cells infected with japonese encephalitis virus. *Virchows Arch. B* 63: 25-36.

Havens Jr WP 1954. Hepatitis, yellow fever, and dengue. *Annu. Rev. Microbiol.* 8: 289-310.

Henchal EA, Gentry MK, McCown JM, Brandt WE 1982. Dengue virus-specific and flavivirus group determinants identified with monoclonal antibodies by indirect immunofluorescence. *Am. J. Trop. Med. Hyg.* 31: 830-836.

Hotta H, Murakami I, Miyasaki K, Takeda Y, Shirane H, Hotta S 1981. Inoculation of dengue virus into nude mice. *J. Gen. Virol.* 52: 71-76.

Huang K-J, Li S-Y L, Chen S-C, Liu H-S, Lin Y-S, Yeh T-M, Liu C-C, Lei H-Y 2000. Manifestation of thrombocytopenia in dengue-2 virus-infected mice. *J. Gen. Virol.* 81: 2177-2182.

Humprey CD, Pittman EE 1974. A simple methylene blue-azure-II basic fuchsin for epoxy-embedded tissue sections. *Stain Technol.* 49: 9.

Jessie K, Fong MY, Devi S, Lam SK, Wong KT 2004. Localization of dengue virus in naturally infected human tissues, by immunohistochemistry and in situ hybridization. *J. Infect. Dis.* 189: 1411-1418.

Johnson AJ, Roehrig JT 1999. New mouse model for dengue virus vaccine testing. *J.Virol.* 73: 783-786.

Juffrie M, Meer DM, Hack CE, Haasnoot K, Sutaryo, Veerman AJ, Thijs LG 2000. Inflammatory mediators in dengue virus infection in children: interleukin-8 and its relationship to neutrophil degranulation. *Infect. Immun.* 68: 702-707.

Lanciotti RS, Calisher CH, Gubler DJ, Chang GJ, Vorndam V 1992. Rapid detection and typing of dengue viruses from clinical samples by using reverse transcriptase-polymerase chain reaction. *J. Clin. Microbiol.* 30: 545-51.

Lawn SD, Tilley R, Lloyd G, Finlayson C, Tolley H, Newmann P, Rice P, Harrison TS 2003. Dengue hemorrhagic fever with fulminant hepatic failure in an immigrant returning to Bangladesh. *Clin. Infect. Dis.* 37: 1-4.

Lee YR, Liu MT, Lei HY, Liu CC, Wu JM, Tung YC, Lin YS, Yeh TM, Chen SH, Liu HS 2006. MCP-1, a highly expressed chemokine in dengue haemorrhagic fever/dengue shock syndrome patients, may cause permeability change, possibly through reduced tight junctions of vascular endothelium cells. *J. Gen. Virol.* 87: 3623-3630.

Lin Y, Liao CL, Chen LK, Yeh CT, Liu CI, Ma SH, Huang YY, Huang YL, Kao CL, King CC 1998. Study of dengue virus infection in SCID mice engrafted with human K562 cells. *J. Virol.* 72: 9729-9737.

Ling LM, Wilder-Smith A, Leo YS 2007. Fulminant hepatitis in dengue haemorrhagic fever. *J. Clin. Virol.* 38: 265-268.

Lum LCS, Lam SK, George R, Devi S 1993. Fulminant hepatitis in dengue infection. *Southeast Asian J. Trop. Med. Public. Hlth.* 24: 467-471.

Meiklejohn G, England B, Lennette EH 1952. Adaptation of dengue virus strains in unweaned mice. *Am. J. Trop. Med. Hyg.* 1: 51-58.

Nath P, Tandon P, Gulati L, Chaturvedi UC 1983. Histological & ultrastructural study of spleen during dengue virus infection of mice. *Indian J. Med. Res.* 78: 83-90.

Paes MV, Barreto DF, Takiya CM, Pinhão AT, Côrtes LMC, Majerowicz S, Barth OM 2002. Ultrastructural aspects of mouse liver infected with dengue-2 virus. *Virus Rev & Res.* 7: 38-46.

Paes MV, Pinhão AT, Barreto DF, Costa SM, Oliveira MP, Nogueira AC, Takiya CM, Farias-Filho JC, Schatzmayr HG, Alves AMB, Barth OM 2005. Liver injury and viremia in mice infected with dengue-2 virus. *Virology* 338: 236-246.

Pinzani M 1995. Hepatic stellate (Ito) cells: expanding roles for a liver-specific pericyte. *J. Hepatol.* 22: 700-706.

Rajapakse S 2011. Dengue shock. *J. Emerg. Trauma Shock* 4: 120-127.

Raut CG, Deolankar RP, Kolhapure RM, Goverdhan MK 1996. Susceptibility of laboratory-bred rodents to the experimental infection with dengue virus type 2. *Acta Virologica* 40: 143-146.

Reed LJ, Muench H 1938. A simple method of stimating fifty percents endpoints. *The Am. J. Hyg.* 27: 493-497.

Reynolds 1963. The use of lead citrate at high pH as an electron opaque stain in electron microscopy. *J. Cell Biol.* 17: 208-212.

Rosen L, Drouet MT, Deubel V 1999. Detection of dengue virus RNA by reverse transcription-polymerase chain reation in the liver and lymphoid organs but not in brain in fatal human infection. *Am. J. Trop. Med. Hyg.* 61: 720-724.

Saikia N, Talukdar R, Singal DK, Chaudhary D, Bhullar SS, Tandon RK 2007. Hepatic calcification following dengue virus-induced fulminant hepatic failure. *Indian J. Gastroenterol.* 26: 90-92.

Sarkar JK, Das BC, Mukherjee KK, Chakrabarti SK 1976. Observation on second heterotypic dengue virus infection in mice. *Indian J. Med. Res.* 63: 1713-1719.

Scheuer PJ, Lefkowitch JH 2000. Liver biopsy interpretation, 4th ed. Ed. Harcourt, Health Sciences. Chapter 18, Electron microscopy and other techniques, p. 345-364.

Shresta S, Sharar KL, Prigozhin DM, Beatty PR, Harris E 2006. Murine model for dengue virus-induced lethal disease with increase vascular permeability. *J. Virol.* 80: 10208-10217.

Seneviratne SL, Malavige GN, de Silva HJ 2006. Pathogenesis of liver involvement during dengue viral infections. *Trans. R. Soc. Trop. Med. Hyg.* 100:608-614.

Thein S, Aung MM, Shwe TN, Aye M, Zaw A, Aye K, Aye KM, Aaskov J 1997. Risck factors in dengue shock syndrome. *Am. J. Trop. Med. Hyg.* 56: 566-572.

World Health Organization, 2002. Fact sheet 117.

Yu CY, Hsu YW, Liao CL, Lin YL 2006. Flavivirus infection activates the XBP1 pathway of the unfolded protein response to cope with endoplasmic reticulum stress. *J. Virol.* 80: 11868-11880.